

Downward Longwave Radiation at the Surface from Satellite Measurements

WAYNE L. DARNELL, SHASHI K. GUPTA¹ AND W. FRANK STAYLOR

Atmospheric Sciences Division, NASA Langley Research Center, Hampton, VA 23665

29 March 1983 and 18 July 1983

ABSTRACT

A new technique is presented for generating downward longwave flux at the Earth's surface from satellite meteorological data and a radiative transfer model. The technique was tested by using TIROS-N data from 41 passes over a ground site covering a period of one month. Satellite-derived fluxes were compared with those measured by a ground-based pyrgeometer during each overpass. The standard error of the satellite-derived fluxes relative to the mean ground-measured values was found to be 6.5%.

1. Introduction

Distribution of radiation balance at the Earth's surface is an important factor in determining the temperature fields at the surface and greatly affects the oceanic and atmospheric circulations. The surface radiation balance (SRB) has been recognized to be as important to the weather and climate studies as that at the top of the atmosphere (NASA, 1979). Considerable effort has been made over the past decade to determine the radiation balance at the top of the atmosphere (Vonder Haar and Soumi, 1971; Raschke *et al.*, 1973; Smith *et al.*, 1977; Jacobowitz *et al.*, 1979). Also, top-of-the-atmosphere (TOA) radiation balance parameters are the subject of the Earth Radiation Budget Experiment (ERBE), a satellite mission to be undertaken by NASA and NOAA during the mid-1980s. By comparison, the effort made to determine the radiation balance at the surface has been modest and mostly devoted to methods for determining the shortwave (SW) component (Raschke and Preuss, 1979; Ellis and Vonder Haar, 1978; Tarpley, 1979; Gautier *et al.*, 1980). Results in all these investigations were compared with ground-based pyranometer measurements, and the agreement was generally within 10%. In contrast with the progress of SW research, estimation techniques for longwave (LW) radiation balance at the surface using satellite data are almost nonexistent. Ellington *et al.* (1980) termed this a glaring deficiency and stressed the need for LW estimation techniques using readily available satellite data.

This note presents a new technique for inferring the downward longwave component of SRB from satellite-determined meteorological data using a radiative transfer model (Gupta, 1983). The technique has been

tested thus far with one month of satellite data. Resulting fluxes are compared with simultaneous ground-measured downward longwave fluxes taken by a wideband pyrgeometer at Ann Arbor, Michigan.

2. Radiative transfer model

Downward radiance at the surface in a direction θ relative to zenith from a plane-parallel clear atmosphere is given by

$$N_s(\theta) = \int_{\tau_{rh}}^1 B_s(T_z) d\tau_{rz}(\theta), \quad (1)$$

where $B_s(T_z)$ is the Planck function at the altitude z , τ_{rz} is the atmospheric transmittance between the surface and altitude z , and h represents the top of the atmosphere. For an overcast atmosphere the downward radiance is given by

$$N'_s(\theta) = B_s(T_c)\tau_{rc}(\theta) + \int_{\tau_{rc}}^1 B_s(T_z) d\tau_{rz}(\theta), \quad (2)$$

where the first term on the right side represents radiation from the cloud base and the second term is the radiation from the atmosphere below the cloud. Assuming that the cloud surface is plane-parallel and radiates as a blackbody in the infrared, the net downward radiance is obtained as the cloud-fraction weighted sum of $N_s(\theta)$ and $N'_s(\theta)$. Corresponding flux densities were obtained using the diffusivity approximation with Eqs. (1) and (2) where $B_s(T_c)$ and $B_s(T_z)$ are substituted in flux density units, and τ_{rc} and τ_{rz} are the flux transmittances obtained by multiplying the corresponding vertical optical depths by the diffusivity factor of 1.66.

The monochromatic Eqs. (1) and (2) were integrated over the 5–50 μm (2000–200 cm^{-1}) range which was divided into 180 spectral intervals, each 10 cm^{-1} wide. Atmospheric transmittance functions for each of these

¹ NASA-NRC Resident Research Associate.

intervals were calculated using the quasi-random band model of absorption (Wyatt *et al.*, 1962). Continuum absorption by water vapor and its temperature dependence were taken into account as outlined by Roberts *et al.* (1976). Flux in the 50–200 μm (200–50 cm^{-1}) region, though small, was computed on the assumption that the atmosphere emits as a blackbody in this region.

Height integration of Eqs. (1) and (2) was carried out by dividing the atmosphere into 50 mb layers. Even though $\approx 99\%$ of the downward surface flux for a clear atmosphere comes from layers below 700 mb, top-of-the-atmosphere in the present model was assumed to be at the 250 mb level. This was because clouds generally can be found up to that level and cloud radiation forms a significant part of the total flux received at the surface. A plot of the downward spectral flux obtained with the present model using mid-latitude clear atmospheric conditions is shown in Fig. 1.

3. Available satellite and ground data

The TIROS Operational Vertical Sounder (TOVS) data, available operationally from NOAA, were found eminently suitable for the present work. The TOVS is a complement of three vertical-sounding instruments that fly aboard NOAA's TIROS-N series of operational meteorological satellites. Data for this study were taken from the TIROS-N satellite (prototype of the TIROS-N series) which operated in a Sun-synchronous orbit of about 854 km altitude at an inclination of about 99° . Orbital coverage was accomplished twice a day at nominal equatorial crossing times of 0300 LST for southbound orbits and 1500 LST for northbound orbits.

Retrieval of meteorological data from the multi-channel soundings of TOVS instruments was accomplished by NOAA using algorithms developed by Smith and Woolf (1976). Characteristics of the TOVS sounding channels and the operational processing techniques

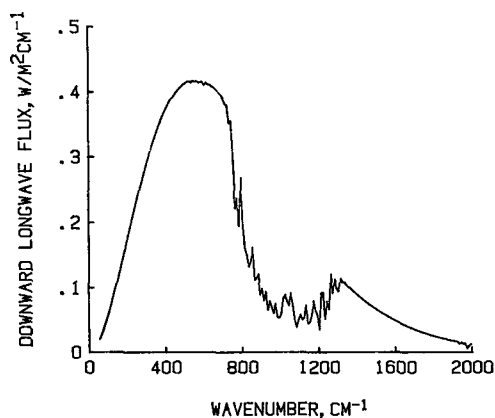


FIG. 1. Spectral distribution of the downward flux for a mid-latitude clear atmosphere in the 50–2000 cm^{-1} (200–5 μm) region.

used by NOAA are discussed by Smith *et al.* (1979). The ground resolution of TOVS soundings extended approximately 300 km along the orbital track and 250–500 km in the crosstrack direction and is referred to as a TOVS box. The operational TOVS data product is comprised of a set of meteorological parameters for each box which contains a surface temperature and pressure, a 15-layer temperature profile covering the troposphere and stratosphere, a 3-layer tropospheric precipitable water profile, fractional cloud cover, cloud-top pressure, and the total ozone burden.

Accuracy of the TOVS data product has been evaluated by comparisons with radiosondes and other measurements. Scoggins *et al.* (1981) have made temperature and water vapor comparisons in south-central United States for 10 April 1979. The radiosonde data were gathered within 1 to 2 hours of the satellite overflight at 20 meteorological stations. Smith *et al.* (1979) have examined differences between TOVS-determined and radiosonde-measured temperature profiles. NOAA has published information on the probable errors in the operational TOVS products (Kidwell, 1981). The errors relevant to the present work are shown in Table 1.

The ground-measured fluxes used for validation of the present technique were obtained from the Solar Energy Measurement Facility, University of Michigan, Ann Arbor. Flux data were in the form of calibrated, continuous strip-chart recordings of the output from an Eppley Precision Infrared Radiometer (PIR). Hourly-averages, centered on the half hour, were taken from the charts and intermediate values centered on the hour were obtained using simple interpolation.

4. Satellite data use

TOVS data sets were preprocessed in two stages before being used in the radiative transfer model to generate the downward longwave surface fluxes. In the first stage, TOVS boxes were selected that were within 2.5° latitude and longitude of the site. Then meteorological parameters from the boxes of each orbit were averaged using an inverse-square site-distance weighting technique.

Second stage preprocessing prepared the orbit-averaged results for the model. Interpolation techniques were used to compute temperature and water vapor values for each 50 mb layer between the surface and 250 mb. For temperature computations, only the bottom six layer temperatures of TOVS were involved. The temperatures for the 50 mb layers were defined at the mean pressure points rather than at the center of each layer. It was assumed that in the altitude range of interest, particularly between successive TOVS layers, the pressure decreases exponentially while the temperature decreases linearly. The temperature T_m corresponding to the mean pressure P_m of the m th 50 mb layer is, therefore, given by

TABLE 1. Probable error in TOVS data products (Kidwell, 1981).

TOVS data product	Probable error
Layer mean temperature: surface to 850 mb	±2.5 K
850 mb to tropopause	±2.25 K
Layer precipitable water	±30%
Cloud cover	±20%
Total ozone: tropical	±15%
polar	±50%

$$T_m = T_n + \left[\frac{T_n - T_{n+1}}{\ln(P_n/P_{n+1})} \right] \ln\left(\frac{P_m}{P_n}\right), \quad (3)$$

where T_n and P_n are the six TOVS temperatures and pressures and P_m lies between TOVS pressure levels P_n and P_{n+1} . The above interpolation procedure was applied to a set of TOVS supplied atmospheric temperatures, and the results are shown in Fig. 2. The plus symbols represent the TOVS derived values, and the open squares the temperatures computed for the boundaries and centers of the 50 mb layers of the model.

The TOVS data specify water burden of the atmosphere in three layers: surface–700 mb, 700–500 mb, and 500–300 mb. The amount of water vapor above 300 mb was considered insignificant. Computation of water vapor for the 50 mb layers was obtained from the orbit-averaged data as follows.

Denoting the total precipitable water in the atmosphere by U_0 , it can be shown (Smith, 1966) that

$$U_0 = \frac{P_0 w_0}{g\beta}, \quad (4)$$

where P_0 is the surface pressure, w_0 the water vapor mixing ratio at the surface, g the acceleration due to

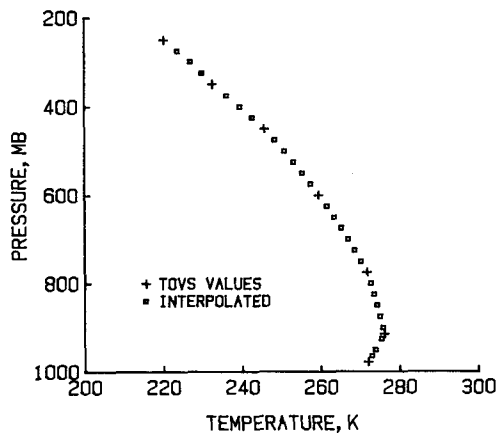


FIG. 2. Temperature profile showing TOVS specified values (plus signs), and those obtained from Eq. (3) at layer boundaries and centers (open squares).

gravity, and $\beta = H/Hw$, where H and Hw are the atmospheric and water vapor scale heights, respectively. If U_1 denotes the precipitable water above the pressure level P_1 , it follows that

$$\frac{U_1}{U_0} = \left(\frac{P_1}{P_0}\right)^\beta \quad (5)$$

and the precipitable water burden of the m th 50 mb layer can be represented as

$$\Delta U_m = U_{m-1} - U_m = U_{m-1} \left[1 - \left(\frac{P_m}{P_{m-1}}\right)^\beta \right]. \quad (6)$$

Values of U_0 (sum of all three layers) and U_1 (sum of upper two layers, $P_1 = 700$ mb) obtained from the TOVS data were used to evaluate the parameter β with Eq. (5), which was then used to calculate the water burdens of the successive 50 mb layers from Eq. (6).

Only total ozone burden of the atmosphere, and not its vertical distribution, is available from TOVS data. Ozone distribution in the altitude range of interest for the model was calculated assuming that it was similar to the distribution for the U.S. Standard Atmosphere (McClatchey *et al.*, 1972). Carbon dioxide, methane, and nitrous oxide were assumed to be uniformly mixed in the atmosphere with volume-mixing ratios of 330, 1.6 and 0.28 ppm, respectively. The effect of aerosols on the downward-infrared flux was not considered in the present work.

Finally, TOVS data give an effective fractional cloud cover and cloud-top pressure; however, fractional cloud cover and cloud-base temperature are the required parameters for computation of downward flux. Since no information regarding cloud thickness is available from TOVS, a nominal cloud thickness of 50 mb was adopted in the present work. At mid-tropospheric altitudes, this corresponds to a geometrical thickness of approximately 700 m. It should be noted that this is in good agreement with estimates of the thickness of middle level clouds (altostratus and altocumulus) for mid-latitudes (Telegadas and London, 1954). Temperature at the cloud base was calculated corresponding to its pressure using Eq. (3). The effect of the 50-mb cloud thickness assumption on the accuracy of the flux results is discussed in the next section.

5. Results and discussion

Satellite-derived downward longwave fluxes were obtained for 41 orbital passes of the satellite over the ground site from 15 April to 15 May 1979. Overpass times were rounded to the nearest half hour to allow direct comparison with the half-hourly ground-measured values. Thus, differences in time-of-measurement between the satellite and pyrgeometer did not exceed about 15 minutes. Comparisons between the satellite-derived and ground-measured fluxes are shown in Fig. 3. These data have a linear correlation coefficient of

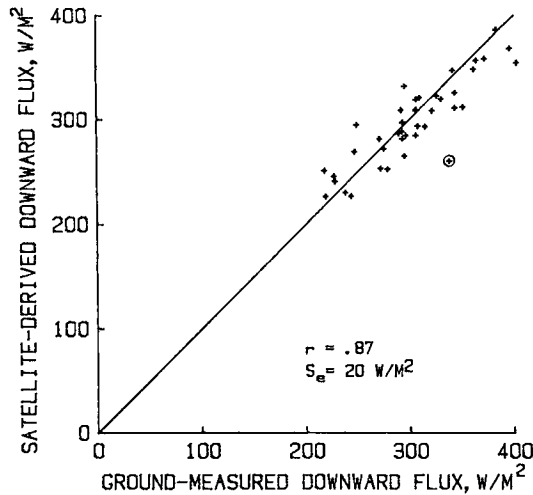


FIG. 3. Comparison of satellite-derived downward fluxes with ground-measured values. The point enclosed in the circle is the one showing >20% error. For a perfect match all data points would be on the diagonal line.

0.87 and a standard error of estimate of 20 W m^{-2} which is 6.5% of the mean value of ground-measured flux. The difference between the mean values of satellite-derived and ground-measured fluxes was 1.9%.

One point (circled on Fig. 3) had more than 20% error and occurred for the nighttime overpass (0354 LST) on 22 April 1979. TOVS data for this orbit indicated only 8% cloud cover at the 750 mb level, while ground observers reported dense ground fog with an undetermined amount of cloud cover. The TOVS processing apparently could not discriminate ground fog radiation from surface radiation, since ground fog will likely appear to TOVS as only a slightly colder surface area. If a very low, 100% cover condition had been input to the radiative model in this case, the resulting computed flux would have been in good agreement with the ground-measured value. Thus, dense fogs or very low clouds may produce significant errors in the satellite-derived fluxes. Additional cloud recognition and quantification problems can occur for multilayer clouds and for thin high clouds.

Flux errors inherent in the technique can be attributed primarily to two causes. The first stems from the use of the relatively coarse spatial resolution of TOVS for characterizing the site meteorology. Most of the radiation entering the pyrgeometer originates from the atmosphere within a few kilometers of the site, while TOVS data give the mean meteorology for a few hundred kilometers about the site. It is clear that for any given overpass, meteorological parameters (i.e., temperature and water vapor profiles, cloud fraction and height) in a small portion of a TOVS box can be considerably different than the mean values for the entire box. Thus, comparisons of local ground-measured fluxes and satellite-derived fluxes that are based on regional meteorology, such as those given in Fig.

3, will inherently suffer from errors caused by spatial variability of the meteorology within the region.

The second primary error source concerns the inherent errors in the TOVS data product. Numerous approximations and computational models are involved in the transformation of the original radiation data. Sensitivity of the satellite-derived fluxes to the probable errors in the TOVS meteorological parameters was examined. The magnitudes of these probable errors were presented in Section 3. Pressure and temperature profiles for the model atmosphere used in this sensitivity study were taken from the U.S. Standard Atmosphere, and the water vapor profile was calculated corresponding to a surface relative humidity of 75% and a β of 4. Cloud cover for this model was assumed to be 50%, and the cloud base was assumed at the 650 mb level. Since TOVS data have no information on the location of cloud base, sensitivity here was evaluated for an arbitrary error of 100 mb. Sensitivity to error in cloud-base height was also evaluated for a lower cloud with base at 800 mb. Results of the sensitivity study are summarized in Table 2. Assuming that all of these errors are uncorrelated and independent, the combined error was estimated by the root-sum-square method, which was found to be about 6.5%, not to be confused with the same value stated earlier for the mean error for satellite-derived fluxes.

6. Concluding remarks

This work is the first effort to use operational satellite data to derive surface radiation budget parameters in the longwave region. The technique has been validated by comparing model-computed fluxes with those measured at the ground.

For clear-sky conditions, approximately 99% of this radiation originates in the atmosphere below 700 mb. Under partly cloudy or overcast conditions, radiation from clouds contributes a significant part of the total flux. Profiles of water vapor and temperature, cloud cover, and cloud-base height are the important parameters affecting this radiation. Except for cloud-base heights, these parameters are available from TOVS data products. Cloud-base heights were estimated from

TABLE 2. Sensitivity of computed flux to probable errors of TOVS data.

TOVS parameter	Probable error	Error in S_i (%)
Surface & tropospheric temperature	$\pm 2.5 \text{ K}$	± 3.0
Water vapor burden of the atmosphere	$\pm 30\%$	± 4.6
Cloud cover	$\pm 20\%$	± 3.1
Cloud base height:		
650 mb	$\pm 100 \text{ mb}$	± 1.29
800 mb	$\pm 100 \text{ mb}$	± 1.35

TOVS-supplied cloud-top heights and climatological values of cloud thicknesses. Sensitivity studies showed this approximation did not produce large errors in the flux results.

Standard error in the results obtained with this technique was found to be 6.5%. This is lower than the errors present in similar surface-radiation studies of the shortwave region. The most significant part of the error arises from the estimation of the local meteorological parameters over the ground-measurement site and from the probable errors in the TOVS meteorological data product. The ground-site comparison is necessary, however, only for the validation of the technique. The long-term objective of this work is to develop a capability for deriving surface radiation budget on a regional scale where it is expected that errors would be smaller.

Acknowledgments. The authors wish to thank Edward Ryznar and Michael R. Weber of the University of Michigan for supplying pyrgeometer records of ground-measured fluxes and for valuable discussions regarding the accuracy of the instrument. Thanks are also due Fred M. Denn of Kentron International for help in processing the data at the NASA Langley Research Center.

REFERENCES

- Ellingson, R. G., F. Bretherton, C. Gautier and K. Katsaros, 1980: Report of the Radiation Working Group. *Proc. of a Workshop on Applications of Existing Satellite Data to the Study of Ocean Surface Energetics*. C. Gautier, Ed., University of Wisconsin-Madison, 185-186.
- Ellis, J. S., and T. H. Vonder Haar, 1978: Solar radiation reaching the ground determined from meteorological satellite data. *Proc. Third Conf. on Atmospheric Radiation*. University of California, Davis, 187-189.
- Gautier, C., G. Diak and S. Masse, 1980: A simple physical model to estimate incident solar radiation at the surface from GOES satellite data. *J. Appl. Meteor.*, **19**, 1005-1012.
- Gupta, S. K., 1983: A radiative transfer model for surface radiation budget studies. *J. Quant. Spectrosc. Radiat. Transfer*, **29**, 419-427.
- Jacobowitz, H., W. L. Smith, H. B. Howell, F. W. Nagle and J. R. Hickey, 1979: The first 18 months of planetary radiation budget measurements from the Nimbus 6 ERB experiment. *J. Atmos. Sci.*, **36**, 501-507.
- Kidwell, K. B., 1981: *NOAA Polar Orbiter Data, (TIROS-N and NOAA-6) Users Guide*. Environmental Data and Information Service, NOAA, 90 pp.
- McClatchey, R. A., R. W. Fenn, J. E. A. Selby, F. E. Volz and J. S. Garing, 1972: Optical properties of the atmosphere. AFCRL-72-0497, 108 pp. [NTIS-AD753075].
- NASA, 1979: *Earth Radiation Budget Science*, 1978: NASA CP-2100, 72 pp. [NTIS-N79-32797].
- Raschke, E., and H. J. Preuss, 1979: The determination of solar radiation budget at the Earth's surface from satellite measurements. *Meteor. Rundsch.*, **32**, 18-28.
- , T. H. Vonder Haar, M. Pasternak and W. R. Bandeen, 1973: The radiation balance of the Earth-atmosphere system from Nimbus-3 radiation measurements. NASA TN D-7249, 73 pp. [NTIS-N73-21702].
- Roberts, R. E., J. E. A. Selby and L. M. Biberman, 1976: Infrared continuum absorption by atmospheric water vapor in the 8-12 μm window. *Appl. Opt.*, **15**, 2085-2090.
- Scoggins, J. R., W. E. Carle, K. Knight, V. Moyer and N.-M. Cheng, 1981: A comparative analysis of rawinsonde and Nimbus 6 and TIROS N satellite profile data. NASA RP-1070, 72 pp. [NTIS-N81-15640].
- Smith, W. L., 1966: Note on the relationship between total precipitable water and surface dewpoint. *J. Appl. Meteor.*, **5**, 726-727.
- , and H. M. Woolf, 1976: The use of eigenvectors of statistical covariance matrices for interpreting satellite sounding radiometer observations. *J. Atmos. Sci.*, **33**, 1127-1140.
- , J. Hickey, H. B. Howell, H. Jacobowitz, D. T. Hileary and A. J. Drummond, 1977: Nimbus 6 Earth radiation budget experiment. *Appl. Opt.*, **16**, 306-318.
- , H. M. Woolf, C. M. Hayden, D. Q. Wark and L. M. McMillin, 1979: The Tiros-N operational vertical sounder. *Bull. Amer. Meteor. Soc.*, **60**, 1177-1187.
- Tarpley, J. D., 1979: Estimating incident solar radiation at the surface from geostationary satellite data. *J. Appl. Meteor.*, **18**, 1172-1181.
- Telegadas, K., and J. London, 1954: A physical model of the Northern Hemisphere tropopause for winter and summer. Scientific Rep. No. 1, Dept. Meteorology and Oceanography, N.Y.U., Contract No. AF19(122)-165, 55 pp.
- Vonder Haar, T. H., and V. E. Soumi, 1971: Measurements of the Earth's radiation budget from satellites during a five-year period. I: Extended time and space means. *J. Atmos. Sci.*, **28**, 305-314.
- Wyatt, P. J., V. R. Stull and G. N. Plass, 1962: Quasi-random model of band absorption. *J. Opt. Soc. Amer.*, **52**, 1209-1217.